Mathematical Institute
University of Oxford

Modelling Neuronal Growth:

Coupling Tubulin Transport with Mechanical Forces in an Elongating Axon

Contents

1 Introduction

1.1 Biology

Though key to understanding how neural networks form and evolve, neuronal growth is a poorly understood process. In the early stages of morphogenesis a neuronal cell consists of the main cell body, known as the soma, and a multitude of protruding dendrites. Eventually, a single dendrite referred to as the axon outgrows the rest. The role of the axon during neurogenesis is to traverse[1] the substrate and extend to form synaptic connections, typically with the dendrites of another neuron. As such the role of dendrites is to receive electrical signals. The axon itself consists of the main shaft and the growth cone. The protein tubulin is created in its soluble form within the soma, and exists in its polymerised form as the main constituent of the cytoskeleton of the axon [1]. Referred to as microtubules, these cross-linked chains of solid, polymerised tubulin are what give the axonal shaft its structural integrity. The growth cone of the axon is the key structure that performs the necessary sensory functions and mediates the motility of the neuron [3]. The cytoskeleton of the growth cone consists predominantly of F-actin.

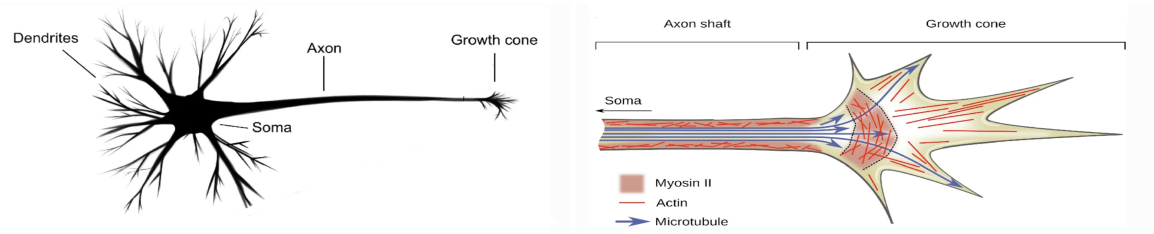

(a) Full schematic of neuron (b) Close up of the axon and growth cone

Figure 1: Schematic of 1a - The full neuron including the dendrites protruding from the soma, along with the dominant axon and its growth cone. And 1b - A close up of the distal end of the axon along with the growth cone.

1.2 Theories of Neuronal Growth

Though we have an understanding of the anatomy of growing neurons, the process by which mass is accumulated during neurogenesis has been highly debated for years.

[1]The traversal of the substrate is known as axon guidance. Though we omit specifics on this process, we note that axon guidance is controlled by sensory properties of the growth cone, at the distal tip of the axon.

Older theories regarding neuronal growth assumed that growth of the axon was dictated mainly by the assembly and disassembly of tubulin into microtubules at the growth cone, a notion we hereon refer to as tip growth. Models of neuronal growth based on these theories typically focus on the transport of soluble tubulin produced at the soma to the growth cone. Though promising, models based solely on the theory of tip growth are highly contested, as it has not been confirmed experimentally, and moreover there have been experiments conducted which disagree with this theory. Newer models of neuronal growth have focused instead on the effects of mechanical forces on growing axons, and in particular how these give rise to a velocity profile throughout the axon, not just at the tip.

We first consider the classical formulation of slow axonal transport of soluble tubulin and tip growth. We then review a more contemporary model which takes into account the mechanical forces, and offers a velocity profile throughout the axon, defying the theory of tip growth. Though the notion of tip growth is highly contested, it cannot be denied that tubulin must be transported along the axon. As such we present an original PDE model governing the transport of soluble tubulin with regard to the mechanics of a growing axon. We offer analytic solutions to a simplified model and numerical solutions to the analytically intractable variants. We confirm numerically that under specific assumptions, our model conforms to the nuances of the aforementioned models in their respective regimes.

2 Model for Transport Mediated Growth

We first consider a transport mediated model of axonal growth. Such models are built on the assumption that elongation of the axon is governed by assembly of microtubules at the tip. Despite the daunting facts about tip growth, not all is lost with such models. Transport should not be neglected as there must be transport of material for the addition of mass, or growth. As such we shall outline the literature regarding these formulations, as a means to incorporate the presented results in our proposed model. In particular we consider the 1D transport model proposed by McLean et al [2]. In such models we desire the profile of the concentration of tubulin along the axon, as this will polymerise into microtubules and mediate the growth of the axon. In this model we consider the concentration of tubulin along the extent of the axon shaft over time, $c(x,t)$. Considering the flow of soluble tubulin within a test volume in the axon, one can arrive at the standard continuity equation that describes the

conservation of tubulin, we have

$$\frac{\partial c}{\partial t}(x,t) + \frac{\partial J}{\partial x}(x,t) = S(x,t). \tag{1}$$

where $J(x,t)$ is the flux of tubulin and $S(x,t)$ denotes a sink/source term. McLean et al [2] models the flux by a combination of diffusion and active transport. We have

$$J(x,t) = \underbrace{-D\frac{\partial c}{\partial x}(x,t)}_{\text{Diffusion}} + \underbrace{ac(x,t)}_{\text{Active transport}}, \tag{2}$$

where D is the diffusion constant and a is the effective active transport velocity. The active transport represents transport against the concentration gradient, a process mediated by motor proteins in the substrate [3]. The diffusion term is simply given by Fick's law. As diffusion acts with the concentration gradient (high to low concentration), we can also refer to this term as the passive transport term. We note that diffusion and active transport act in opposite directions, hence the difference in signs. We take the sink term $S(x,t)$ to account for the degradation of tubulin along the axon, meaning the tubulin that decays before it can polymerise. We let $S(x,t) = -\kappa c(x,t)$, where κ is the constant rate of decay. Substituting in the flux and sink terms gives the PDE that governs the transport of tubulin along the axon:

$$\frac{\partial c}{\partial t}(x,t) - D\frac{\partial^2 c}{\partial x^2}(x,t) + a\frac{\partial c}{\partial x}(x,t) = -\kappa c(x,t). \tag{3}$$

The proximal boundary condition is prescribed arbitrarily as some sufficiently large time dependent concentration[2] $\tilde{c}_S(t)$, namely we have $c(0,t) = \tilde{c}_S(t)$. To obtain an expression for the rate of elongation, we need to prescribe a distal boundary condition that accounts for both the assembly of tubulin into microtubules for growth, and the dissassembly of tubulin which increases the pool of available tubulin for growth. If we denote by ϵ_l and ζ_l constants related to assembly and disassembly of tubulin respectively, we enforce the following distal moving flux boundary condition:

$$\frac{\partial c}{\partial x}(l(t),t) = -\epsilon_l c(l(t),t) + \zeta_l. \tag{4}$$

The Stefan condition (4) can be formulated into the following expression for the rate of growth of the axon;

$$\frac{1}{e}\frac{\mathrm{d}l}{\mathrm{d}t}(t) = k^+ c(l(t),t) - k^-. \tag{5}$$

[2]We note that this is not the only option for the proximal boundary condition; several options have been used in the literature however we only consider this one as it shall also be used in our proposed model.

where we have the consumption of tubulin at rate k^+ and disassembly of tubulin at rate k^-. Here e denotes the typical elongation due to the addition of one tubulin dimer[3]. The exact form of 5 is perhaps not as important as understanding that this equation simply says that growth ($\mathrm{d}l/\mathrm{d}t$) is a function of the concentration of tubulin at the tip only. This idea is to some extent disproved in the experiment conducted by Zheng et al. [5], where the researchers towed axons of chick sesnory neurons with a needle. They observed the resultant extended neuron, correcting for any possible elastic stretching so as to solely determine how the axons grew under the towing force. The results of this experiment showed that marked mitochondria throughout the axon moved in the direction of the applied force. If tip growth were to be the correct theory, then we would expect all the mitochondria, except at the tip, to remain stationary.

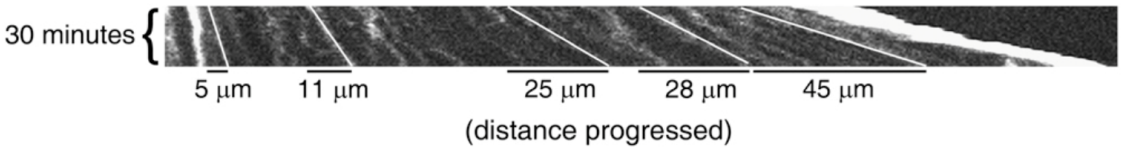

Figure 2: Chemograph showing the motion of marked mitochondria throughout the axon over a period of 30 minutes. (O'toole et al. [4])

The results of the experiment are shown in figure 2. We notice that there is growth at each point along the axon, with what appears to be faster growth towards the growth cone. This motivates the necessity of a model which captures the mechanical effects of a growing axon, which we present next.

3 Model for Mechanically Mediated Growth

We next discuss the mechanically mediated growth model by O'toole et al. [4]. This model considers the axon as a viscoelastic material in contact with an adhesive substrate. Essentially this means that the axon demonstrates properties of both viscous fluids and elastic solids, and exists in a substrate that induces a friction force due to adhesion opposing the motion of the axon during growth. In this model we consider the effects of a constant towing force, F_0 applied at the growth cone over a period of time. We derive how such a force would induce a velocity profile across the length of

[3]Simply put, this refers to the average increase in length of microtubules on addition of a unit amount of tubulin.

the axon that depends both on the magnitude of this applied force and also on the specific viscoelastic properties of the axon. Implicitly in this we include the resultant opposing force induced by adhesion from the substrate. By modelling the axon as a series of dashpots, we expect a dissipative system where the velocity and force profiles decay exponentially from the growth cone towards the soma. We denote by g the axial viscosity, by η the friction constant and by G the growth dashpot constant. Both g and η have dimensions of viscosity. We note that g is large when the number of microtubules or the amount of cross linking between them is high, and η is high when the strength of adhesion between the axon and the substrate is high. The dashpot constant characterises the response of the axon to the constant force applied at the growth cone. It therefore makes sense that G is proportional to g and the cross sectional area A, i.e, $G = gA$. In this model we assume that the dissipation of F_0 along the axon is characterised by the constant η, and that during the elongation, the diamater of the axon remains constant (so G remains constant) and hence there is no thinning but instead just the addition of mass to increase the length.

We now follow and elaborate the derivation of the decaying velocity profile by O'toole et al. [4]. Given an applied towing force at the growth cone, F_0, we denote by $f(x, l(t))$ and $v(x, l(t))$ the force and velocity profiles along the axon respectively. It is important to note that these are functions of both position along the axon and the current length of the axon. The applied force causes a distension at each point due to the dashpot model, and the change in velocity between two infinitesimally far points is inversely proportional to the dashpot constant (since it acts to give a constant velocity in the high G limit) and proportional to the force at that point, i.e.

$$\frac{\partial v}{\partial x}(x, l(t)) = \frac{1}{G} f(x, l(t)). \tag{6}$$

Integrating (6) gives

$$v(x, l(t)) = \int_0^x \frac{1}{G} f(s, l(t)) \mathrm{d}s. \tag{7}$$

The frictional relationship can be given as a change in dissipation forces at each point x, namely we have

$$\frac{\partial f_\eta}{\partial x}(x, l(t)) = -\eta v(x, l(t)) \tag{8}$$

where f_η is the dissipative force (the amount by which F_0 is reduced as a consequence of the friction). We note the inclusion of the negative sign as a consequence of most of the force being dissipated at the soma and none being dissipated at the growth

cone. Integrating (8) from the growth cone to the point x gives the total dissipation over that part of the axon;

$$\begin{aligned} f_\eta(x, l(t)) &= \int_{l(t)}^{x} \frac{\partial f_\eta}{\partial p}(p, l(t))\mathrm{d}p \\ &= \int_{x}^{l(t)} \eta v(p, l(t))\mathrm{d}p \\ &= \frac{\eta}{G}\int_{x}^{l(t)}\int_{0}^{s} f(p, l(t))\mathrm{d}p\mathrm{d}s \end{aligned}$$

where we have simply substituted in the expression for $v(x, l(t))$ from (7). Since the effective force at some position is given by the reduction of F_0 by the dissipation, namely $f(x, l(t)) = F_0 - f_\eta(x, l(t))$, we have

$$f(x, l(t)) = F_0 - \frac{\eta}{G}\int_{x}^{l(t)}\int_{0}^{s} f(p, l(t))\mathrm{d}p\mathrm{d}s. \tag{9}$$

Differentiating (9) twice gives the PDE

$$\frac{\partial^2 f}{\partial x^2}(x, l(t)) - \frac{\eta}{G} f(x, l(t)) = 0 \tag{10}$$

to which we also prescribe the boundary conditions $f(l(t), l(t)) = F_0$ and $\partial f/\partial x(0, l(t)) = 0$. The first of these conditions ensures the force at the tip is F_0 and the second enforces a constant local force at the soma. Implicit in our model is that the velocity profile evaluated at the growth cone is just the rate of elongation, formally we have

$$\frac{\mathrm{d}l}{\mathrm{d}t}(t) = v(l(t), l(t)). \tag{11}$$

Differentiating (9) once gives

$$\begin{aligned} \frac{\partial f}{\partial x} &= \frac{\eta}{G}\int_{0}^{x} f(p, l(t)\mathrm{d}p \\ &= \eta v(x, l(t)). \end{aligned}$$

Rearranging and substituting in (11) gives us an expression for the rate of elongation in terms of the force:

$$\frac{\mathrm{d}l}{\mathrm{d}t}(t) = \frac{1}{\eta}\frac{\partial f}{\partial x}(l(t), l(t)). \tag{12}$$

We also prescribe the initial condition to this ODE; $l(0) = l_0$ where l_0 is just the initial length of the axon. We can solve (10) with the prescribed boundary conditions to give the force profile along the length of the axon given F_0, we have

$$f(x, l(t)) = F_0 \frac{\cosh\left(x(\eta/G)^{1/2}\right)}{\cosh\left(l(t)(\eta/G)^{1/2}\right)}. \tag{13}$$

Then, we can insert this expression for the force profile into (12) and solve with the prescribed initial condition to get an expression for the time dependent length of the axon, we have

$$l(t) = \left(\frac{G}{\eta}\right)^{1/2} \sinh^{-1}\left(\beta \exp\left(\kappa t\right)\right), \tag{14}$$

where we define the constants $\beta := \sinh\left(L_0\left(\eta/G\right)^{1/2}\right)$ and $\kappa := F_0/G$. Finally we can use the relationship $v = \eta^{-1}(\partial f/\partial x)$ to obtain the velocity profile. We have

$$v(x, l(t)) = \frac{F_0}{(\eta G)^{1/2}} \frac{\sinh\left(x\left(\eta/G\right)^{1/2}\right)}{\cosh\left(l(t)(\eta/G)^{1/2}\right)} \tag{15}$$

4 Coupled Model

We are now in a position to couple the one dimensional transport limited and mechanically mediated models as presented in the previous sections. We do this by employing the continuity equation (1) that governs the transport of tubulin across the length of the axon. We encompass the behaviour of tubulin transport resulting from a constant towing force F_0 by introducing additional flux and sink terms which we shall motivate. We have, just as in the transport model,

$$\frac{\partial c}{\partial t}(x,t) + \frac{\partial J}{\partial x}(x,t) = S(x,t). \tag{16}$$

Where now we incorporate flux and source/sink terms that encompass both the transport of tubulin and the effects of the towing force. In our model we take

$$J = J_d + J_a + J_v \tag{17}$$

where, just as in the transport model we have $J_d = -D(\partial c/\partial x)$ and $J_a = ac$ as the passive (diffusion) and active transport terms respectively. The final term J_v accounts for the additional influx of tubulin into an arbitrary test volume due to the bulk motion induced by the towing force. As described in the previous section this force gives rise to a velocity field and hence we have additional contribution to the transport of tubulin as a function of the position and current length of the axon. It follows that this contribution is given by

$$J_v = v_{\text{ad}} c(x,t) = \frac{F_0}{(\eta G)^{1/2}} \frac{\sinh\left(x\left(\eta/G\right)^{1/2}\right)}{\cosh\left(l(t)(\eta/G)^{1/2}\right)} c(x,t) \tag{18}$$

where we have simply substituted in the velocity profile given by (15), using the notation v_{ad} to emphasise that this is a prescribed velocity field and not an unknown

in the problem. Substituting these flux terms in gives the total flux

$$J = -D\frac{\partial c(x,t)}{\partial x} + ac(x,t) + v_{\text{ad}}c(x,t). \tag{19}$$

Next we consider the sink terms. We could take

$$S = S_d + S_c \tag{20}$$

where $S_d = -\kappa c(x,t)$ would represent the decay of tubulin, as in the transport model by McLean et al.[2], however for simplicity we ignore this term. Instead we have $S = S_c$ where S_c arises from the mechanical forces involved. Under the application of the constant towing force F_0 we expect point-wise stretching of the axon to occur, that is a stretch at each point x in the domain. In accordance with this stretch, we enforce that the supply of tubulin for growth is sufficient such that the lineal density of the axon remains constant, that is the width of the axon does not change. We can model this with a continuity equation for the solid part of the axon where we have polymerised tubulin. We have

$$\frac{\mathrm{d}}{\mathrm{d}t}\int_{\mathbf{V}} \rho \, d\mathbf{V} = \int_{\partial V} \rho v_{ad} \, dS + \int_{\mathbf{V}} S_c(x,t) \, d\mathbf{V} \tag{21}$$

for an arbitrary test volume V. This equation states that the rate of change of density of polymerised tubulin ρ in some test volume V is equal to the density loss due to narrowing of the polymerised tubulin plus some source of polymerised tubulin. The key term here is the boundary flux - this arises from the velocity profile within the axon that comes from the stretching. In this case the point x in the axon is pulled by the bulk motion, which is governed by the velocity profile v_{ad}, giving rise to the boundary flux ρv_{ad}. To construct our model, we enforce that the sink term S_c is sufficient to counteract the narrowing of the axon, namely we want to find S_c such that ρ is constant. Applying the divergence theorem to the boundary term, we arrive at the continuity equation for polymerised tubulin:

$$\frac{\partial \rho}{\partial t} = \frac{\partial(\rho v_{ad})}{\partial x} + S_c(x,t).$$

With the additional constraint that the density ρ remains constant, we find

$$S_c(x,t) = -\rho\frac{\partial v_{ad}}{\partial x}. \tag{22}$$

Substituting the flux and sink terms into the continuity equation (16), we arrive at the full PDE governing the transport and mechanics. We have

$$\frac{\partial c}{\partial t}(x,t) + \frac{\partial}{\partial x}\left(-D\frac{\partial c}{\partial x}(x,t) + ac(x,t) + v_{ad}c(x,t)\right) = -\rho\frac{\partial v_{ad}}{\partial x}, \tag{23}$$

for points (x,t) in the domain

$$\Omega_{xt} = \{(x,t) : (x,t) \in [0, l(t)] \times [0, \infty)\}. \tag{24}$$

The PDE is first order in time and second order in space so we also require one initial condition and two boundary condition to close the problem. At the proximal boundary we enforce some arbitrary concentration which is perhaps not easily found *a priori*. To this end we shall consider 'optimal' choices for this profile. At the distal (moving) boundary we prescribe a no flux boundary condition so as to enforce no penetration of tubulin through the axon. Hence the boundary conditions are

$$c(0,t) = c_S(t), \tag{25}$$

$$\frac{\partial c}{\partial x}(l(t),t) = \frac{a + v_{\text{ad}}(l(t),t)}{D} c(l(t),t) \tag{26}$$

where we can determine the proximal $c_S(t)$. The no flux boundary condition is derived from equating $J = J_d + J_a + J_v = 0$ for $x = l(t)$. We note that this is for the case $D \neq 0$; in the case $D = 0$ the no flux boundary condition simplifies to $c(l(t),t) = 0$. As in the model by Mclean et al. [2], we enforce the simplest initial conditions that satisfies both of these boundary conditions, in this case we have the exponential profile for $D \neq 0$

$$c(x,0) = c_S(0) \exp\left(\frac{a}{D} x + \frac{F_0(\cosh\left(x\left(\eta/G\right)^{1/2}\right) - 1)}{GD\cosh\left(l_0\left(\eta/G\right)^{1/2}\right)} \right) \tag{27}$$

where $l_0 = l(0)$. This is easily derived after integrating the velocity profile. In the case $D = 0$, the initial condition that satisfies both boundary conditions is simply the linear profile $c(x,0) = c_S(0)(1 - x/l_0)$.

We can take values of constants[4] from the respective papers of each of the models reviewed in sections 2 and 3. From McLean et al's model [2] we have $a = 2.3\text{mm/day}$ and $D = 8.6\mu\text{m}^2\text{s}^{-1}$. From O'toole's model [4] we have $G = 3.9 \times 10^7 \mu\text{mh}^{-1}$, $\eta = 9.6 \times 10^3$ Pa s, $F_0 = 200\mu$dynes. The literature provides little insight into the value of the lineal microtubule density ρ, as such, we take $\rho = 1\text{kgm}^{-1}$ for the sake of argument[5].

[4]We convert the given values to standard SI units: $a = 2.7 \times 10^{-8}\text{ms}^{-1}$, $D = 8.6 \times 10^{-12}\text{m}^2\text{s}^{-1}$, $G = 0.011\text{ms}^{-1}$, $\eta = 9.6 \times 10^3\text{Pa s}$, $F_0 = 2 \times 10^{-9}$N and $\rho = 1\text{kgm}^{-1}$.

[5]We stress that this prescibed value of ρ is likely not physical.

4.1 Analytic Solutions

In the simplified steady-state[6], no diffusion case we can solve our model analytically. The model simplifies to

$$\frac{\mathrm{d}}{\mathrm{d}x}\left(ac(x;T) + v_{\mathrm{ad}}(x;T)c(x;T)\right) = \frac{\mathrm{d}}{\mathrm{d}x}\left(-\rho v_{\mathrm{ad}}(x;T)\right), \tag{28}$$

$$c(0;T) = c_S(T), \tag{29}$$

$$c(l(t);T) = 0, \tag{30}$$

$$c(x;T=0) = c_S(0)\left(1 - \frac{x}{l_0}\right) \tag{31}$$

where we note that we are considering the particular solution at time $t = T$, thus T is a parameter and not a variable. Since we are considering a steady state solution it is perhaps more appropriate to recognise the effect of increasing the parameter T as considering the concentration along a longer axon. Solving (28) together with (30) gives

$$c(x;T) = \frac{\rho(v_{\mathrm{ad}}(l(t);T) - v_{\mathrm{ad}}(x;T))}{a + v_{\mathrm{ad}}(x;T)}, \tag{32}$$

from which we deduce that $c_S(T) = \rho v_{ad}(l(t);T)/a$ by enforcing (29).

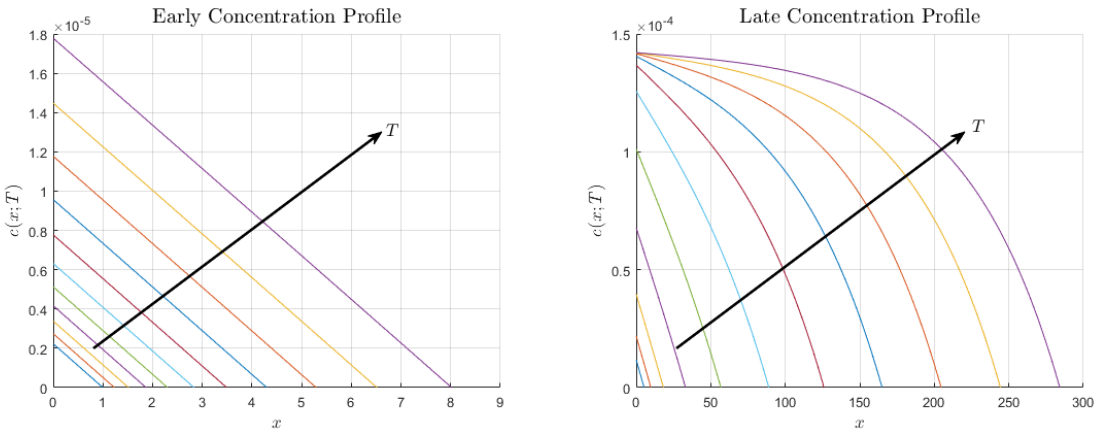

(a) (b)

Figure 3: Steady-state concentration profiles in the absence of diffusion for varying time parameter. 3a Early time (short axon), where we observe a linear decay along the axon. 3b Late time (longer axon), where the concentration drastically drops in the neighbourhood of the growth-cone.

[6]It is important to note that taking the steady state in our case is justified by the fact that metabolic processes are faster than growth, and so we have a seperation of timescales.

We see in figure 3 the concentration profiles for small and large time parameter T, i.e. for increasing axon length. We see a linear concentration profile for lower values of T as expected, with a build up of tubulin in the vicinity of the growth cone in the large T limit. This shows that longer axons experience a 'build up' of tubulin which gets closer and closer to the growth cone for larger axons. The limiting case here is clearly a constant concentration profile along the axon.

4.2 Numerical Solutions

Including diffusion into the steady-state equation gives rise to a analytically intractable system, which for all practical applications is suitably analysed numerically. In this case we have the system

$$D\frac{\mathrm{d}^2c}{\mathrm{d}x^2}(x;T) - (a + v_{\mathrm{ad}}(x;T))\frac{\mathrm{d}c}{\mathrm{d}x}(x;T) - (c+\rho)\frac{\mathrm{d}v_{\mathrm{ad}}}{\mathrm{d}x}(x;T) = 0, \tag{33}$$

$$c(0;T) = c_S(T), \tag{34}$$

$$\frac{\mathrm{d}c}{\mathrm{d}x}(l(t);T) = \frac{a + v_{\mathrm{ad}}(l(t);T)}{D}c(l(t);T), \tag{35}$$

$$c(x;T=0) = c_S(0)\left(1 - \frac{x}{l_0}\right). \tag{36}$$

Here we can find the optimal concentration at the soma such that we have 'just enough' tubulin available throughout the axon. Namely we find $c_S(T)$ under the additional constraint $c(l(t);T) = 0$, which replaces the no flux boundary condition.

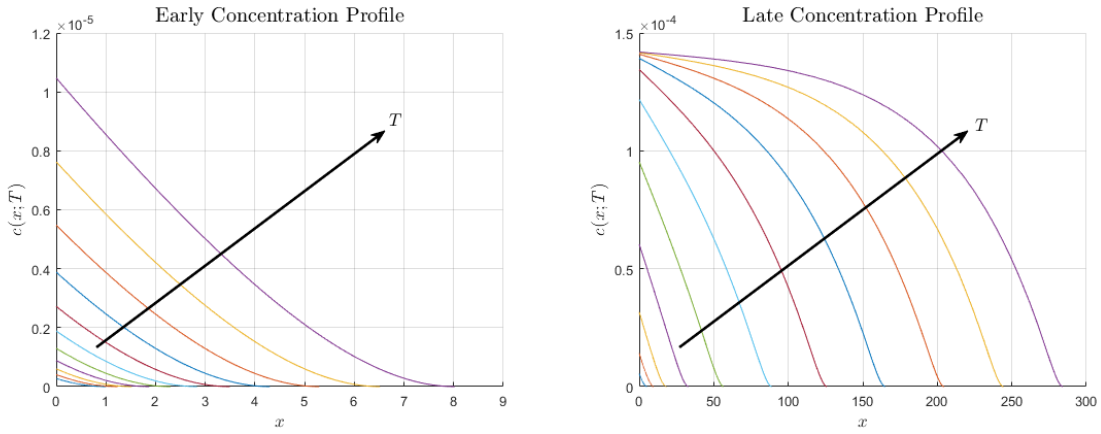

(a) (b)

Figure 4: Numerical solutions of the steady-state concentration profiles in the presence of diffusion for varying time parameter. 4a Early time concentration profile, where we observe a linear decay along most of the axon with increasing gradient towards the growth cone. 4b Late time concentration profile, where the concentration drastically drops close of the growth-cone, with increasing gradient in the neighbourhood of the growth cone.

From figure 4 we see a very similar concentration profile to the analytic solution that neglects diffusion, the key difference being the flattening of the profile towards the distal boundary. This is simply a consequence of adding another form of transport that acts to decrease the areas of high concentration.

4.2.1 Full PDE

We next solve numerically the full time dependent model for the case $c(l(t), t) = 0$. The problem becomes

$$\frac{\partial c}{\partial t}(x,t) + \frac{\partial}{\partial x}\left(-D\frac{\partial c}{\partial x}(x,t) + ac(x,t) + v_{ad}c(x,t)\right) = -\rho\frac{\partial v_{ad}}{\partial x}, \tag{37}$$

$$c(0,t) = c_S(t), \tag{38}$$

$$c(l(t),t) = 0, \tag{39}$$

$$c(x,0) = c_S(0)\left(1 - \frac{x}{l(0)}\right), \tag{40}$$

$$\Omega_{xt} = \{(x,t) : (x,t) \in [0, l(t)] \times [0,\infty)\}. \tag{41}$$

and we can resolve the issue of the moving boundary condition (39) by rescaling to a stationary domain. The substitution $x = yl(t)$ yields

$$\frac{\partial \tilde{c}}{\partial t} = \frac{D}{l^2}\frac{\partial^2 \tilde{c}}{\partial y^2} - \frac{1}{l}\left(a + \tilde{v}_{\text{ad}} - y\frac{\mathrm{d}l}{\mathrm{d}t}\right)\frac{\partial \tilde{c}}{\partial y} - \frac{1}{l}\left(\tilde{c} - \rho\right)\frac{\partial \tilde{v}_{\text{ad}}}{\partial y}, \tag{42}$$

$$\tilde{c}(0,t) = \tilde{c_S}(t), \tag{43}$$

$$\tilde{c}(1,t) = 0, \tag{44}$$

$$\tilde{c}(y,0) = \tilde{c_S}(0)\left(1 - y\right), \tag{45}$$

$$\Omega_{yt} = \{(y,t) : (y,t) \in [0,1] \times [0,\infty)\}. \tag{46}$$

Where $\tilde{c} = \tilde{c}(y,t) = c(yl(t),t)$ and $\tilde{v}_{\text{ad}} = \tilde{v}_{\text{ad}}(y,t) = v_{\text{ad}}(yl(t),t)$ for all $y \in [0,1]$.

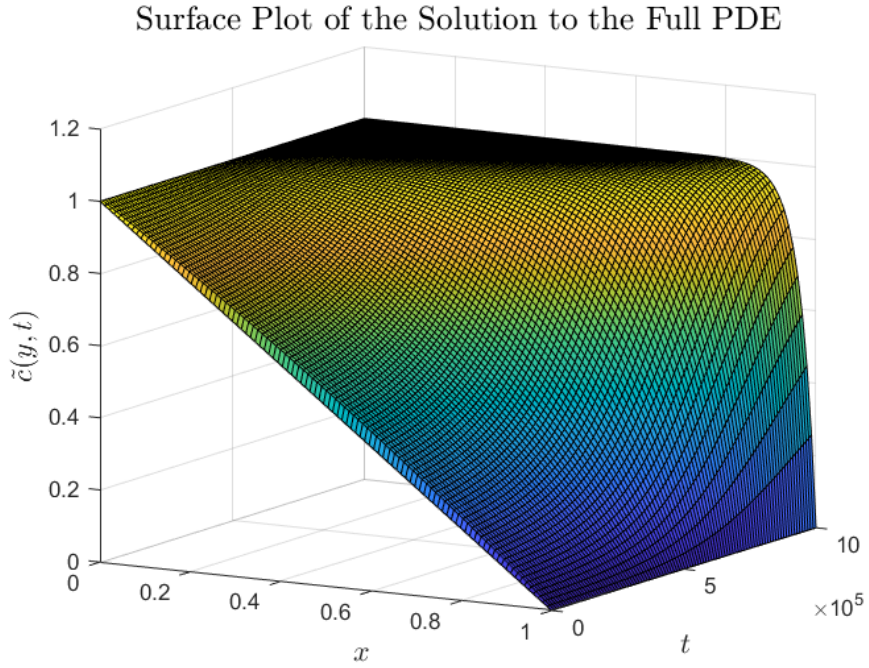

Figure 5: Numerical solution of the full rescaled PDE with prescribed boundary and initial conditions for $\tilde{c_s} = 1$.

Even for this simplified rescaled model, we see corresponding behaviour with the previous simulations. We see that for early times, the concentration profile is linear and for later times it becomes more constant with a steep drop of concentration at the growth cone. This, again is indicative of a build up of soluble tubulin starting at the soma and tending towards the growth cone for later times. It should be noted that the choice of $\tilde{c_s} = 1$ was made for convenience in the numerical scheme, nonetheless it suffices to show a temporal concentration profile consistent with the steady state

solutions. The fact that we see similar trends in both the full PDE and the steady state ODE further backs our justification of taking a steady state solution - there is indeed a separation of timescales between metabolic process and growth.

4.3 Limiting Cases

We next investigate the limiting cases of the model in its steady state. Namely we show that the coupled model simplifies to each of its comprising models in their respective regimes. We show that enforcing an inverse proportional relationship between η and G does indeed return the expected relationship in each limiting case. We begin with the steady state model. We have the second order in space ODE

$$-D\frac{\mathrm{d}^2c}{\mathrm{d}x^2} + (a + v_{\mathrm{ad}})\frac{\mathrm{d}c}{\mathrm{d}x} + (c + \rho)\frac{\mathrm{d}v_{\mathrm{ad}}}{\mathrm{d}x} = 0. \tag{47}$$

We perform the transformation $x \to L\tilde{x}$ where L has dimensions of length and $\tilde{x}$ is dimensionless. We can now define the dimensionless parameter $\epsilon := L(\eta/G)^{1/2}$, and let

$$\alpha := \frac{F_0}{(\eta G)^{1/2}}$$

where we enforce that ηG is constant (and hence α is constant). Here ϵ is the parameter we shall vary in the limiting cases. Substituting these into the ODE after setting $L = 1$ and dropping tildes for convenience gives

$$-D\frac{\mathrm{d}^2c}{\mathrm{d}x^2} + \left(a + \alpha\frac{\sinh(\epsilon x)}{\cosh(\epsilon l(t))}\right)\frac{\mathrm{d}c}{\mathrm{d}x} + (c + \rho)\epsilon\alpha\frac{\cosh(\epsilon x)}{\cosh(\epsilon l(t))} = 0 \tag{48}$$

after using the expression for the velocity profile given by (15). We analyse this ODE at time $t = 1$, where $l := l(1)$. We also prescribe the boundary conditions

$$c(l, 1) = 0 \tag{49}$$

$$\frac{\mathrm{d}c}{\mathrm{d}x}(l, 1) = 0. \tag{50}$$

The first of these ensures an 'optimal' concentration profile, and the second follows from the first after enforcing no flux at the growth cone. We solve (48) together with boundary conditions (49) and (50) numerically for limiting cases of ϵ.

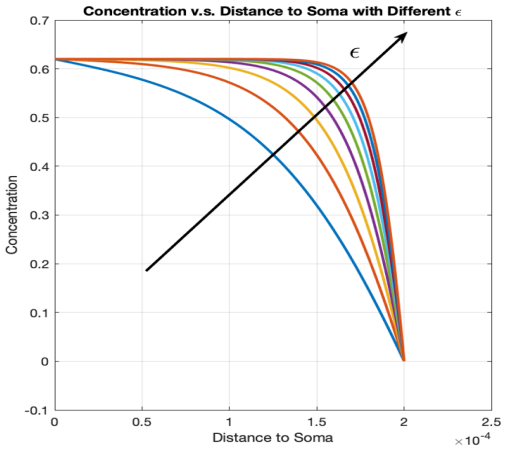

(a) $D = 0$

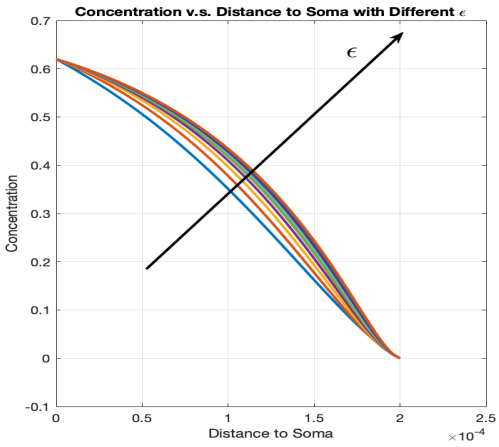

(b) $D > 0$

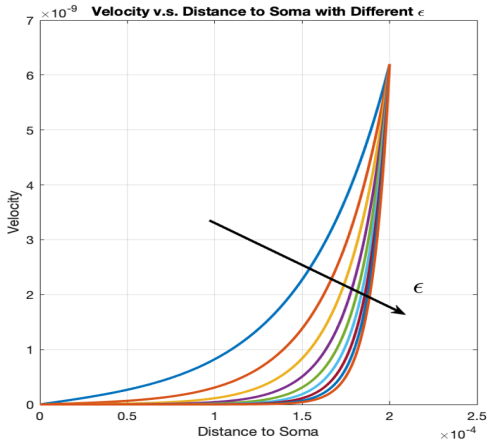

(c) Velocity Profile

Figure 6: Asymptotic concentration and velocity profiles with and without diffusion. 6a: Concentration profile in the absence of diffusion. 6b: Concentration profile with diffusion. 6c Velocity profile

In the limiting case $\epsilon \to \infty$ we have that $\eta \gg G$ which implies that the relative effect of adhesion dominates the resistance of the axon to the towing force. As such when the constant towing force is applied at the tip, friction overpowers the axon's ability to stretch and F_0 is fully dissipated close to the growth cone - this is nothing but the assumption in the tip growth formulation of axonal growth. It follows that we would expect the velocity profile to emulate a delta function centered at $x = l(t)$. We indeed see this delta function like behaviour of the velocity profile for increasing ϵ in figure 6. Physically, this result shows that in the regime of the transport model considered in section 2, the velocity profile reduces to zero except at the tip - i.e,

we recover tip growth. We also see the concentration profile for increasing ϵ, which becomes more steep towards the growth cone, with a constant profile along the axon. This indicates that tubulin is consumed solely at the growth cone in the regime of the transport model, again agreeing with the notion of tip growth. In the limiting case $\epsilon \to 0$ we have that $G \gg \eta$ which is indicative of a strong linking between dashpots relative to the dissipative forces under a constant towing force. This is the regime in which mechanical effects have a significant effect and as such the velocity profile varies along the axon due to the dissipative forces and strong linking between dashpots. The concentration profile in this regime is closer to linear as expected since now growth occurs at each point along the axon and as such tubulin is consumed throughout. These results verify that our coupled model satisfies both the mechanical model and the transport model when restricted to their respective regimes. We note that this analysis works only under our assumption that α is constant and so η is inversely proportional to G.

5 Concluding Remarks

We have motivated the necessity for aspects of both transport limited and mechanically mediated models of axonal growth, noting in particular that although tip growth may not be correct, the need for tubulin transport is still present in a growing axon. We have reviewed and offered a coupling between a transported limited model of axonal growth, along with a model that incorporates the mechanical forces involved. Through both numerical and analytic analysis we have shown that our model provides a reasonable concentration profile along the axon taking into account an applied towing force, both in the time dependent and steady state scenarios. Finally we have shown that our model simplifies to each of the separate models when casting the problem to their respective regimes. An obvious extension to our work would be to investigate how growth is effected by transport effects in the mechanical model, since technically our model only offers a one-way coupling of the effects that mechanical forces have on the transport of tubulin through the axon. One possible extension to our model would be to consider the regime of early neurogenesis in which there are several competing dendrites. One could also consider comparing our results with real data on axons to verify (or refute) aspects of our model.

References

[1] R. B. Maccioni and V. Cambiazo. "Role of microtubule-associated proteins in the control of microtubule assembly". In: *Physiological Reviews* 75.4 (1995). PMID: 7480164, pp. 835–864. DOI: 10.1152/physrev.1995.75.4.835. eprint: https://doi.org/10.1152/physrev.1995.75.4.835. URL: https://doi.org/10.1152/physrev.1995.75.4.835.

[2] Douglas R. McLean and Bruce P. Graham. "Mathematical formulation and analysis of a continuum model for tubulin-driven neurite elongation". In: *Proceedings of the Royal Society of London. Series A: Mathematical, Physical and Engineering Sciences* 460.2048 (2004), pp. 2437–2456. DOI: 10.1098/rspa.2004.1288. eprint: https://royalsocietypublishing.org/doi/pdf/10.1098/rspa.2004.1288. URL: https://royalsocietypublishing.org/doi/abs/10.1098/rspa.2004.1288.

[3] Hadrien Oliveri and Alain Goriely. "Mathematical models of neuronal growth". In: *Biomechanics and Modeling in Mechanobiology* 21.1 (2022), pp. 89–118. ISSN: 1617-7940. DOI: 10.1007/s10237-021-01539-0. URL: https://doi.org/10.1007/s10237-021-01539-0.

[4] Matthew O'Toole, Phillip Lamoureux, and Kyle E. Miller. "A Physical Model of Axonal Elongation: Force, Viscosity, and Adhesions Govern the Mode of Outgrowth". In: *Biophysical Journal* 94.7 (2008), pp. 2610–2620. ISSN: 0006-3495. DOI: https://doi.org/10.1529/biophysj.107.117424. URL: https://www.sciencedirect.com/science/article/pii/S0006349508705149.

[5] J Zheng et al. "Tensile regulation of axonal elongation and initiation". en. In: *J Neurosci* 11.4 (Apr. 1991), pp. 1117–1125.